

Castor Oil-based Polyurethanes Containing Cellulose Nanocrystals

V.M. Wik,^{1,2} M.I. Aranguren,¹ M.A. Mosiewicki¹

¹ *Institute of Materials Science and Technology (INTEMA), University of Mar del Plata - National Research Council (CONICET), Av. Juan B. Justo 4302, Mar del Plata 7600, Argentina*

² *Department of Fibre and Polymer Technology, Royal Institute of Technology, Stockholm S-100 44, Sweden*

Partially foamed and nanocellulose-reinforced polyurethanes (PU) based on castor oil (CO) were prepared and their different properties were measured and related to their structures. A castor oil-based polyol (COPO) was obtained by alcoholysis of CO with triethanolamine. The COPO was used in the preparation of partially foamed and solid PU. Cellulose nanofibrils (NC) in the range of the rheological percolation content were incorporated to the materials and the final mechanical properties of these nanocomposites were analyzed. The incorporated NC considerably affected the rheology of the suspensions, which presented solid-like behavior under frequency sweep tests with the addition of only 0.5 wt% of NC. By increasing the NC concentration the dispersion becomes increasingly difficult. The properties of the solid PU were also affected by the incorporation of NC and a significant increase of the tensile modulus was observed for the 0.5 wt% NC composite, compared to the unfilled solid PU. This behavior was associated to the incorporation of the rigid particle reinforcement and the interfacial bonding. As expected, the partially foamed PU showed lower modulus than the corresponding solid PU. *POLYM. ENG. SCI.*, 51:1389–1396, 2011. © 2011 Society of Plastics Engineers

INTRODUCTION

Increasing environmental concern and economical factors around the world have been driving efforts for searching and using alternative raw materials in the polymer industry. In particular, polyurethanes (PU), offering a broad variety of properties that are useful in different areas of applications, are very interesting materials that can be prepared from reactants obtained from renewable resources of wide availability.

The use of castor oil (CO) as polyol replacement in polyurethane (PU) formulations has been reported by several authors. Isocyanate containing reactants can be reacted with the hydroxyl groups in the CO, which are naturally present in the chemical structure of this particular vegetable oil. Ricinoleic acid having one hydroxyl group (at C12) and one carbon–carbon double bond (at C9) per molecule is the main fatty acid in the composition of this oil [1]. However, the original concentration of hydroxyl reactive groups is not enough to obtain rigid PU, and the chemical modification of the oil was considered. Among other possibilities, the alcoholysis reaction with glycerin or triethanolamine (TEA) is a possible route of modification to increase the hydroxyl groups in the oil structure [2–4].

It is widely known that the addition of microfibers of high modulus to a polymeric matrix can improve its mechanical properties, specially its stiffness. In the last years, the research interest on the study of different polymeric systems containing nanosize particles has been growing, because a polymer containing a low concentration of well-dispersed nanoparticles can largely increase its modulus (with respect to the unfilled material). In particular, the introduction of nanosize fillers into different polyurethane matrices has been previously reported: functionalized graphene sheet has been efficiently dispersed in thermoplastic polyurethane matrices [5–7]. Moreover, Marcovich et al. [8] have reported the use of cellulose nanocrystals obtained by acid hydrolysis in a rubbery PU matrix at concentrations below 5 wt%. Cellulose is one of the most abundant materials in the nature, has a low cost and good mechanical properties [9–10]. In recent years, several studies have reported on the incorporation of different types of cellulose nanofibers in polymeric matrices with significant modification of the materials performance [11–15].

The aim of the present work has been to synthesize a polyol from CO to be used in the production of rigid PU. Two different systems were prepared and characterized: a lightly foamed material and a solid (unfoamed) one. The

Correspondence to: M.A. Mosiewicki; e-mail: mirna@fi.mdp.edu.ar

Contract grant sponsor: National Research Council of Republic Argentina (CONICET); Science and Technology National Promotion Agency–National University of Mar del Plata (ANPCyT–UNMdP).

DOI 10.1002/pen.21939

Published online in Wiley Online Library (wileyonlinelibrary.com).

© 2011 Society of Plastics Engineers

effect of adding different contents of cellulose nanocrystals into the solid polyurethane was also analyzed.

EXPERIMENTAL

Materials

The utilized polyol was obtained by alcoholysis of CO (Parafarm[®], Argentina, hydroxyl value = 169.3 mg KOH g⁻¹) with TEA (>99%, Laboratorios Cicarelli, Argentina). Lithium hydroxide (>99%, Fluka) was used as catalyst.

For the preparation of the rigid PU, the used isocyanate reactant was a 4,4'-diphenylmethane diisocyanate prepolymer, pMDI (Rubinate 5005, Huntsman Polyurethanes, equivalent weight of 131 g eq⁻¹).

The molar ratio of NCO to OH groups was adjusted to 1.1 for each system.

Cellulose nanofibrils (NC) were obtained from commercial microcrystalline cellulose (Avicel PH-101, FMC Bio-Polymer) by acid hydrolysis using a method described in a previous work and were incorporated to the polymer formulation as reactive reinforcements [8]. Crystallites of cellulose obtained from acid hydrolysis have been previously characterized [8], resulting in nanofibers with about 67% of crystallinity, diameters between 10 and 15 nm and aspect ratios from 10 to 15. The cellulose nanocrystals (NC) were dispersed in the COPO by sonication and pMDI was further incorporated and mixed. The NC and the COPO were dried in a vacuum oven (at 60°C and 80°C, respectively) until constant weight before being used.

Synthesis of COPO

The lithium hydroxide, dried CO and TEA were mixed together in a stirred reactor. The temperature was raised to 150°C in 0.5 h and then maintained at this value for 2.5 h. The CO/TEA molar ratio was 1/3, and the catalyst was added as 0.2% by total weight of reactants. The molar excess of TEA is necessary to shift the reversible reaction toward the products. A scheme of the chemical reaction is presented in Fig. 1. The final product is a complex mixture of components, because polyols based on the glycerol or the TEA are possible and any of these species can contain 0, 1, 2, or 3 fatty acids chains per molecule. Previous studies indicate that the main components are species containing one or two fatty acid chains [16–18].

Preparation of Partially Foamed and Solid Materials

In an attempt to achieve rigid partially foamed PU (low-density PU), the COPO was directly mixed with the pMDI. No water was added because no extensive foaming was intended. The polyol and pMDI were mechanically mixed for 20 s, and the mixture was poured in a metal mould of 14 cm of internal diameter and closed. This was

done rapidly to maintain foaming to a minimum and then, the mould was put in a press under 4 MPa, heated to 70°C and held for half an hour in these conditions, which lead to materials with few and small bubbles. This limited foaming, which is the result of the remaining humidity of the reactants (even after drying under vacuum), is useful in reducing the weight of the composites.

For the preparation of the solid materials, the oil-based polyol (containing 0, 0.5, 1.0, or 3 wt% NC) was dissolved in tetrahydrofuran (THF). This step was necessary to reduce the initial reaction rate when the pMDI was added to the system. THF was then allowed evaporating from the open mould. The mould was closed and the samples were cured as indicated for the slightly foamed materials. Samples of about 1 mm thick were obtained in both cases.

Rheological Characterization of the NC-Polyol Suspensions

The rheological properties of dispersions of 0, 0.5, 1, 2, and 3 wt% of NC in COPO were determined at room temperature using an Anton Paar, Physica MCR 301 rheometer. Cone and plate geometry (diameter 25 mm) was chosen to measure the viscoelastic response of the suspensions. A low strain of 0.2 % (linear viscoelastic region) was used to measure the storage modulus as a function of frequency for the different suspensions.

Polyurethane Characterization

Fourier Transform Infrared Spectroscopy. The technique of transmission was used to characterize the unreinforced polyurethane. The spectra were recorded at 2 cm⁻¹ resolution using a Genesis II Fourier transform infrared spectrometer (FTIR). Reported results are the averages of 16 scans.

Density. The experimental densities were determined by pycnometry in degassed distilled water at room temperature. The duration of the test is sufficiently short to neglect water absorption.

The experimental densities were compared with the theoretical values calculated from the rule of mixture, as follows:

$$\frac{1}{\rho_{\text{composite}}} = \frac{W_{\text{solidPU}}}{\rho_{\text{solidPU}}} + \frac{W_{\text{cellulose}}}{\rho_{\text{cellulose}}} \quad (1)$$

where ρ indicates density and W weight fraction. The solid polyurethane density (ρ_{solidPU}) measured experimentally was equal to 1.177 g cm⁻³, whereas the cellulose density was taken from the literature as 1.56 g cm⁻³ [19].

Additionally, using the density of the solid material (ρ_{solidPU}) and that of the partially foamed one (ρ_{foamedPU}), it is possible to calculate the volume fraction of

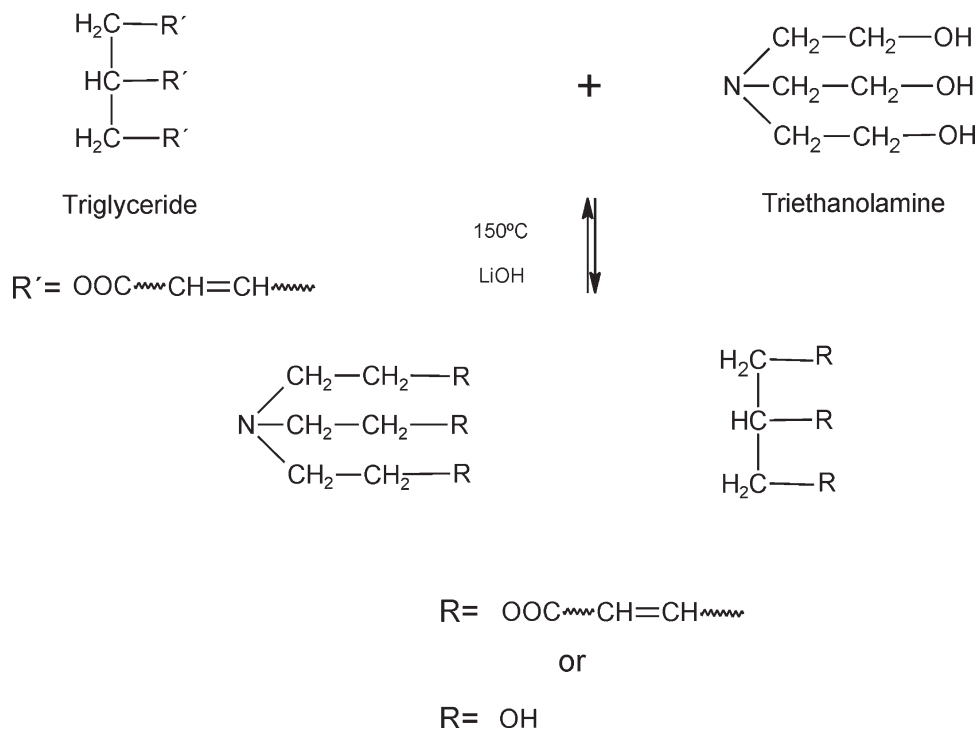


FIG. 1. Scheme of the alcoholysis reaction.

voids (V_v) in the last one according to the following equation [20]:

$$V_v = \frac{\rho_{\text{solidPU}} - \rho_{\text{foamedPU}}}{\rho_{\text{foamedPU}}} \quad (2)$$

Scanning Electron Microscopy. The partially foamed and solid materials were analyzed using scanning electron microscopy (SEM; SEC Philips model SEM 505) on the cryogenic fracture surfaces. The objective was to analyze possible differences in the morphologies of the unfoamed samples (solid) containing different concentrations of NC, as well as the cell structure (shape and size) of the partially foamed material. The samples used for the microscopy study were taken from the broken pieces of the tensile test specimens.

Thermogravimetric Analysis. Thermogravimetric tests for the unreinforced and reinforced PU were performed using a Thermogravimetric analysis (TGA)-50 SHIMADZU Thermogravimetric Analyzer at a heating speed of $10^\circ\text{C min}^{-1}$ under nitrogen atmosphere.

Dynamic-Mechanical Analysis. To study the viscoelastic behavior of the solid materials, a Perkin Elmer dynamic mechanical analyzer, DMA 7e, with tensile bar geometry and continuous nitrogen flow was used. The specimens were cut to approximately $20 \times 5 \times 1 \text{ mm}^3$, linear dimensions. The dynamic and static stresses were kept at 200 and 240 kPa, respectively. The frequency of

the forced oscillations was fixed at 1 Hz, and the heating rate was of $10^\circ\text{C min}^{-1}$. At least two replicate determinations were made to ensure the reproducibility of results.

Tensile Testing. Uniaxial tensile tests were carried out in an INSTRON 8501 Universal testing machine, according to the ASTM D638-94. Specimens from each sample were cut using a dog-bone-shaped driller and tested at a crosshead speed of 1 mm min^{-1} . Four specimens of each sample were tested. The elastic tensile modulus, the stress, and deformation to rupture were calculated from the obtained stress-strain curves.

The presence of some foaming affects the properties of the PU, by reducing their mechanical properties. According to the theoretical study reported by McKenzie [21], the modulus (E) of a material containing voids (partially foamed polyurethane) can be estimated knowing the modulus of the solid material (unfoamed sample) and the volume fraction of voids as follows:

$$E_{\text{foamedPU}} = E_{\text{solidPU}} \cdot (1 - V_v)^2 \quad (3)$$

where V_v is the void volume fraction.

RESULTS AND DISCUSSION

Rheology of the NC-Polyol Liquid Suspensions

The rheological characterization of dispersions of the oil-based polyol with different NC content was performed (Fig. 2). The neat polyol curves are not shown in the

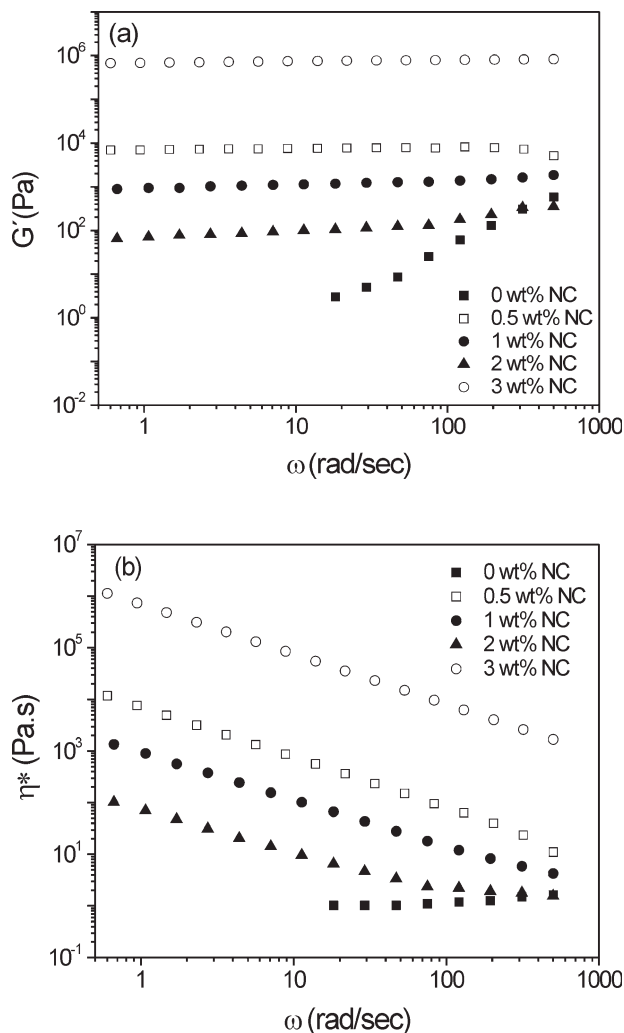


FIG. 2. Rheological properties of the nanocrystals-polyol liquid suspensions. a) Shear storage modulus versus frequency. b) Complex viscosity versus frequency.

complete range, because of the low quality of the signal at low frequencies. The shear storage modulus (G') as a function of frequency for the COPO with 0, 0.5, 1, 2, and 3 wt% of nanocrystals is shown in Fig. 2a. It is clear that G' increases significantly with the incorporation of NC. The neat polyol shows the typical behavior of a viscoelastic liquid and, consequently, there is no equilibrium modulus at low frequencies. On the contrary, all the suspensions show equilibrium modulus, a typical solid-like behavior, even at the lowest concentration (0.5 wt%). Additionally, in the range of small strains considered in these tests, the 0.5 and 1 wt% dispersions present modulus essentially independent of the frequency in the analyzed frequency range, as in a strong gel-like system. The presence of the nanocrystals restricts the polyol relaxation, leading to the observed solid-like viscoelastic behavior. Previous investigations have shown that the addition of about 1 wt% of cellulose nanocrystals to a commercial polyol resulted in a suspension that also showed an

equilibrium modulus at low frequencies. This rheological response was explained because the concentration of the cellulose crystals in the suspension was above the critical percolation threshold [8].

The 2 wt% dispersion shows some frequency dependence at high frequencies, but it also reaches a plateau at low frequencies. Although the behavior shows the characteristics of solid-like behavior, it is clearly below the response of the dispersion containing 0.5 and 1 wt% NC. This is attributed to dispersion problems due to the relatively high concentration of particles (partial aggregation of the nanofibers) [8]. Above this critical concentration, good dispersion becomes very difficult, the nanofibrils can agglomerate, and, thus, the interaction with the polyol is closer to that of a microsuspension instead of a nanosuspension. For higher percentages (3 wt%), the storage modulus presents the highest value. The packing of the agglomerated particles increases and the interactions among aggregates become the largest contribution to the suspension modulus.

Figure 2b presents the complex viscosity versus frequency curves. The natural polyol presents a constant viscosity in the whole range of frequencies investigated. The addition of NC increases the complex viscosity mainly in the low-frequency zone. The addition of only 0.5 wt% NC increases the complex viscosity around 400 times with respect to the unfilled polyol viscosity measured at 20 rad s^{-1} . The dispersions show power law behavior at low frequencies, and, consequently, there is no low-frequency plateau. However, there is a plateau at high frequencies that approaches the value of the constant viscosity displayed by the unfilled polyol. The samples prepared with 1 and 2 wt% of nanocrystals show the dispersion problems mentioned before with a considerable decrease in viscosity, although still exhibiting power law behavior at low frequencies. The sample with 3 wt% of NC presents the highest viscosities in all the frequency range attributed to the interactions of agglomerated particles.

FTIR of the Cured Polyurethane Samples

Figure 3 shows the FTIR spectrum of the unreinforced polyurethane. The spectrum shows all the peaks that are a signature of the presence of urethane chemical groups: at $1700\text{--}1760 \text{ cm}^{-1}$, the urethane carbonyl absorption (NH--CO--O), at 1730 cm^{-1} the free CO--O stretching, and at 1605 cm^{-1} the bonded CO--O stretching and the C--O stretch near 1220 cm^{-1} . The presence of a broad absorbance peak at 3300 cm^{-1} and the peak at 1531 cm^{-1} , assigned to the N--H stretching and N--H bending, respectively, corroborates the existence of the secondary amine of the urethane linkage [22].

Additionally, the isocyanate absorption (--NCO) at 2200 cm^{-1} is not observed indicating that all the isocyanate groups are consumed in the polymerization reaction.

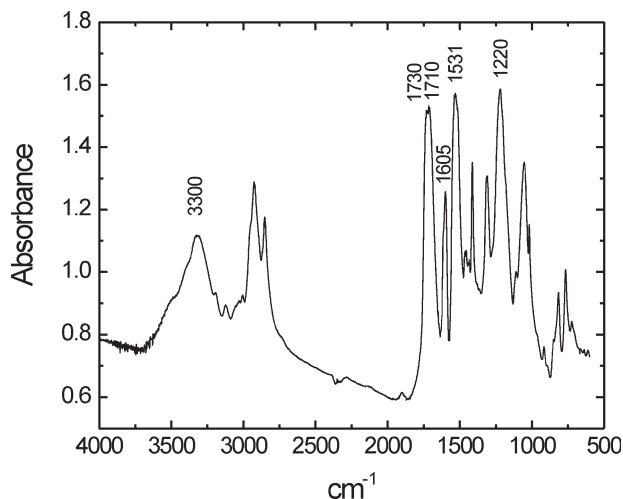


FIG. 3. FTIR spectrum of the polyurethane.

Density of the Cured Materials

Table 1 summarizes the experimental and theoretical density values of the solid materials. Although the amount of nanocrystals added to the PU is very small (0.5 and 1.0 wt%), it is clear that the density increases with the addition of rigid particles. The experimental values are in very good agreement with the theoretical values denoting a negligible volume fraction of voids in these composite materials. As it was expected, the low-density material shows a lower density than the solid PU due to the presence of air bubbles generated in the curing process. The void volume fraction, V_v , calculated from Eq. 2 is 0.243.

SEM of the Cured Samples

Figures 4a–d show the surface micrographs of the solid tensile-tested samples. The images clearly illustrate that the matrix is not foamed in good agreement with the density results mentioned above. The micrograph corresponding to the unreinforced solid PU presents the characteristic appearance of a fragile fracture. The roughness of the surfaces increases with the cellulose content, indicating increased energy dissipation during fracture due to the presence of the nanoparticles. Plastic deformation can be observed in the reinforced materials because the presence of rigid particles offers obstacles to the advance of the crack, which must find new paths for growing, contributing to increase the surface roughness.

Figure 4e shows the fracture surface of the unreinforced low-density PU, where spaced bubbles (partial foaming) confirm the low-density values measured by picnometry.

TGA of the Cured Samples

The weight-loss curves of NC, unreinforced polyurethane, and polyurethane with 1 wt% of NC is presented in Fig. 5.

The thermal decomposition curve of NC shows that the initial weight loss occurs below 160°C corresponding to the removal of humidity and traces of inorganic compounds from the sample. Some components start to break down at about 160°C, whereas cellulose degradation occurs between 300 and 500°C [23].

In turn, the thermal degradation of the PU is a complex mechanism that occurs through several degradation steps [24–26]. There is an initial dissociation of the polymer into polyol and isocyanate components, followed by thermal decomposition that leads to the formation of amines, small transition components, and carbon dioxide [24–25].

The reinforced polyurethane presents curves similar to that of the neat crosslinked polymer at least until 400°C. However, at temperatures more than 400°C, the polyurethane with 1 wt% NC present higher residual mass than the neat polyurethane. Apparently, the reaction between pMDI and the hydroxyl groups in the NC originates new bonds, which give higher thermal stability to the composite materials [25].

Dynamic–Mechanical Analysis of the Cured Samples

The solid materials were analyzed by DMA. Figure 6 show the dynamical tensile storage modulus divided by the glass modulus of each sample at 20°C as a function of temperature for the unreinforced polyurethane and composites containing 0, 1, and 3 wt% NC. It is clear that the matrix presents a broad glass-rubber transition zone that begins near room temperature. All curves show the typical modulus drop related to the glass transition of the materials.

According to the results shown in Fig. 6, the incorporation of NC shifts the dynamic–mechanical curves toward higher temperatures. These results indicate a very strong interfacial interaction between the nanofibers and the matrix. Previous studies have shown that the large increase in glass transition temperatures occurs due to the chemical reaction that takes place between the hydroxyl groups in the particles and the isocyanate groups of the pMDI [8, 17, 18]. Higher amounts of nanocrystals and, consequently, larger surface availability for developing

TABLE 1. Density values of the solid PU composites and partially foamed PU.

Samples	Experimental density (g cm^{-3})	Calculated density (g cm^{-3})
0 wt% NC	1.177 ± 0.026	
0.5 wt% NC	1.219 ± 0.015	1.221
1.0 wt% NC	1.223 ± 0.013	1.226
Partially foamed PU (0 wt% NC)*	0.892 ± 0.105	

* Volume fraction of voids, $V_v = 0.243$.

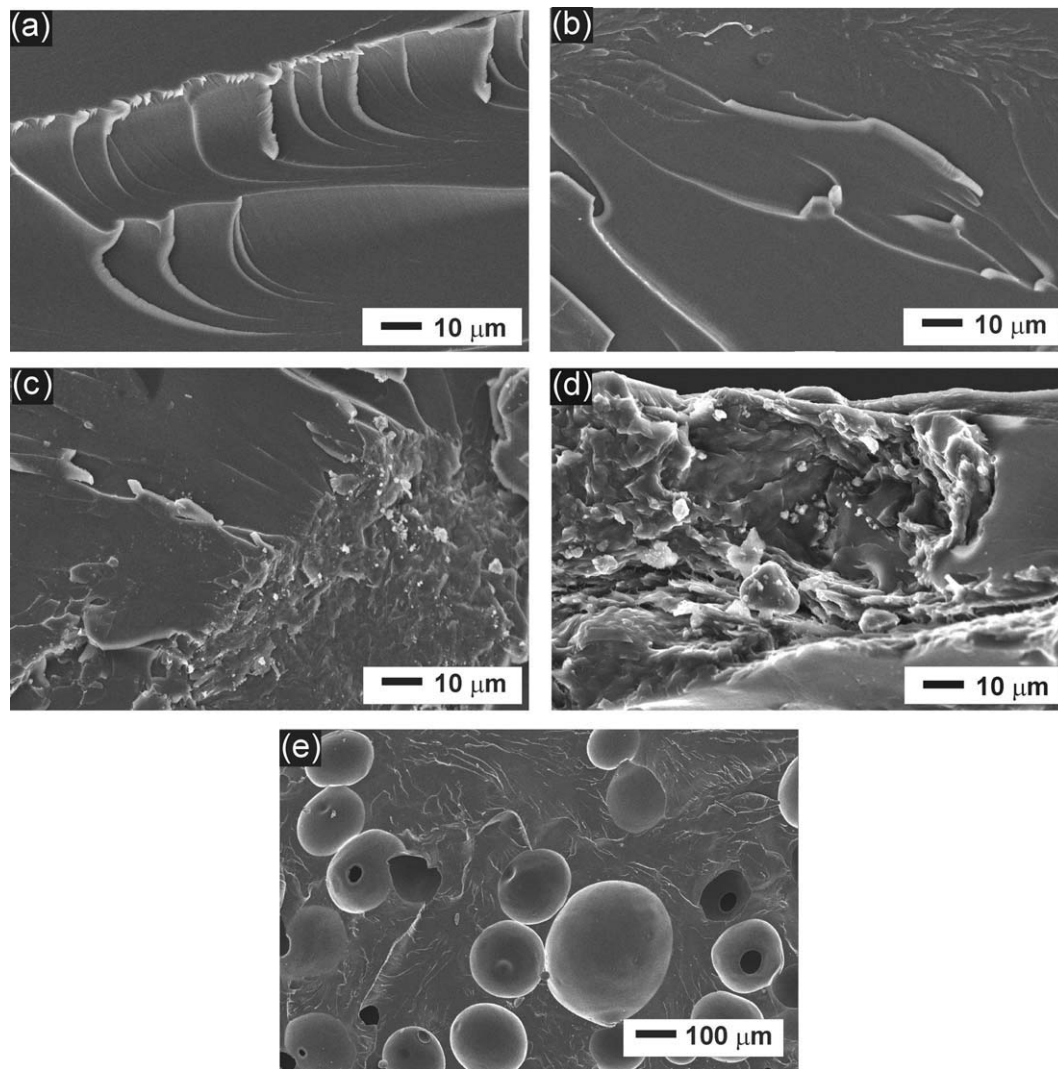


FIG. 4. SEM micrographs of fragile fracture. (a) Solid PU sample containing 0% NC. (b) Solid PU sample containing 0.5% NC. (c) Solid PU sample containing 1.0% NC. (d) Solid PU sample containing 3.0% NC. (e) Unreinforced partially foamed PU.

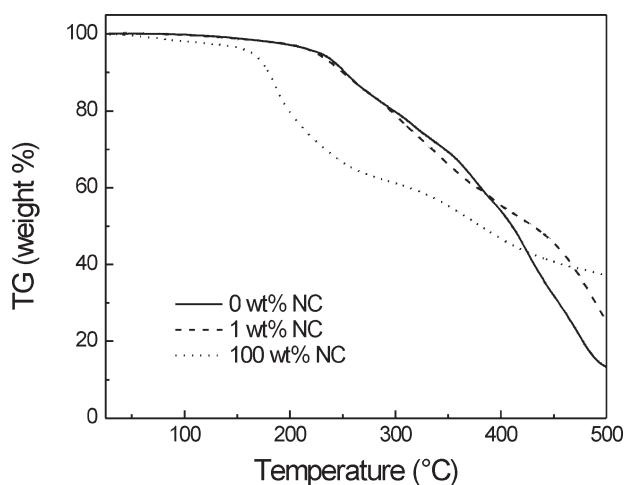


FIG. 5. Thermogravimetric behavior of NC, unreinforced polyurethane and polyurethane with 1 wt% NC.

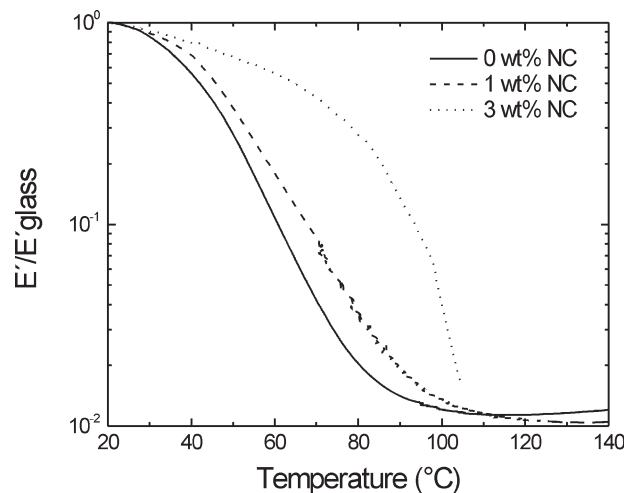


FIG. 6. Dynamic-mechanical properties of the solid NC-PU composites.

interactions with the polymer reduce the mobility of the matrix, and, consequently, its curves move to higher temperatures [8, 17, 18]. The large effect of the addition of 1 wt% of NC in the unreacted liquid polyol has been already discussed: the storage modulus became almost independent of the frequency with the addition of the cellulose crystals. The changes observed are remarkable considering the small cellulose concentrations used in this study.

Tensile Testing

Tensile tests were performed on the solid and partially foamed materials, and the determined stress versus strain curves are shown in Fig. 7, whereas the main mechanical properties are summarized in Table 2. The incorporation of the NC in the solid materials noticeably increases the tensile modulus. The addition of 0.5 wt% of NC to the PU increases the modulus in 32.7%. This improvement can be attributed to the contribution of well-dispersed rigid particles and the interfacial reaction that increases the matrix rigidity. The incorporation of 1 wt% of NC results in a composite with a modulus a 42% higher than that of the unfilled PU. Although this is an important increase, it is clear that the largest incremental change occurred by addition of a minimum NC concentration (0.5 wt%), in agreement with the already discussed DMA results.

The yield stress occurs at the start of the plastic response of the material. At this point, the material reaches its maximum stress and starts to yield (indicated by black arrows in Fig. 7). The materials did not show a clear yield point, but rather a broad change from linear to nonlinear behavior. The beginning of the nonlinear response in general shifts to higher stresses and deformations as more NC is incorporated to the composite. However, the 0.5 wt% sample suffers early failure. The results of deformation at break show that addition of NC in the solid composites decreases the final deformation. The material becomes more rigid and loses extensibility as NC is incorporated, which is the usual behavior when rigid particles of high modulus are added into a polymer matrix.

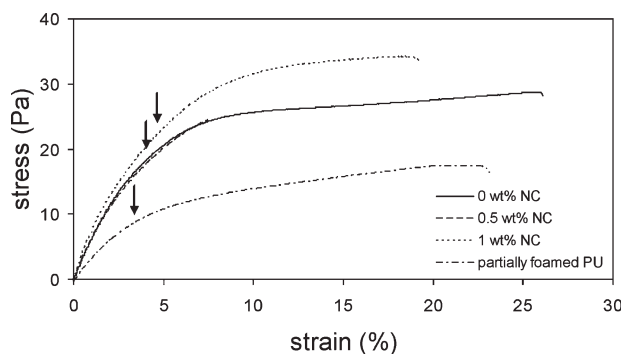


FIG. 7. Tensile stress-strain curves for the solid NC-PU composites.

TABLE 2. Tensile properties of the solid PU composites and partially foamed PU.

Samples	Tensile Modulus, E (MPa)	Stress at break, σ_b (MPa)	Deformation at break, ϵ_b (%)
0 wt% NC	479.5 \pm 43.1	27.6 \pm 0.8	23.5 \pm 3.9
0.5 wt% NC ^a	636.4 \pm 66.3	19.2 \pm 4.0	4.9 \pm 1.8
1.0 wt% NC	682.9 \pm 69.1	31.2 \pm 4.3	11.5 \pm 6.3
Partially foamed PU	292.8 \pm 23.5	17.4 \pm 0.4	19.3 \pm 2.8
(0 wt% NC)	275.5 ^b (calc.)		

^a The samples broke early and the yield phenomena could not be observed.

^b Calculated value (Eq. 3).

The unfilled-and-partially foamed material shows lower tensile modulus than the solid materials. However, foaming did not substantially affect the extensibility (in comparison to the solid unfilled material).

Taking into account that the partially foamed material presents 24.3% of void volume (as calculated and discussed in density section), the modulus for this material is predicted to be 275.5 MPa (calculated from Eq. 3), in good agreement to the experimental value reported in Table 2.

Summarizing, the incorporation of NC increased the stiffness of the material while decreasing its extensibility. By allowing some foaming to occur, the material suffers a decrease of the stiffness but without appreciable change in its extensibility.

CONCLUSIONS

The rheological behavior of a liquid suspension of NC in COPO at a concentration as low as 0.5 wt% showed solid-like response, where the storage modulus resulted independent of the frequency in a dynamic oscillatory test. The differences between the considered suspensions suggest that dispersion problems may be present at higher concentrations. Partially foamed and solid PU were prepared successfully. The use of a solvent to reduce the initial reaction rate is necessary to obtain unfoamed PU. The density increase of the composites with the addition of the cellulose nanocrystals can be predicted by a simple rule of mixture. The incorporation of the NC in the formulation of the polyurethane composites results in changes in the fracture surface roughness as the nanocrystals deviate the path of the advancing crack. The shift of the dynamic-mechanical curves to higher temperatures with the incorporation of minimal quantities of NC is the result of the strong interaction of the cellulose nanocrystals and the PU matrix. The tensile modulus of the composites increases significantly with the incorporation of NC, but the elongation at break decreases. The partially foamed material shows lower modulus than the corresponding solid polyurethane, and this decrease can be predicted by considering the void volume fraction of the sample.

REFERENCES

1. M.W. Formo, E. Jungermann, F.A. Norris, and N.O.V. Sonntag, *Bailey's Industrial Oil and Fat Products*, Vol. 1, 4th ed., Wiley, New York, 453 (1985).
2. S.N. Khot, J.J. Lascala, E. Can, S.S. Morye, G.I. Williams, G.R. Palmese, S.H. Kusefoglou, and R.P. Wool, *J. Appl. Polym. Sci.*, **82**, 703 (2001).
3. R. Tanaka, S. Hirose, and H. Hatakeyama, *Biores. Tech.*, **99**, 3810 (2007).
4. Y.H. Hu, Y. Gao, D.N. Wang, C.P. Hu, S. Zhu, L. Vanoverloop, and D. Randall, *J. Appl. Polym. Sci.*, **84**, 591 (2002).
5. D.A. Nguyen, Y.R. Lee, A.V. Raghu, H.M. Jeong, C.M. Shin, and B.K. Kim, *Polym. Int.*, **58**, 412 (2009).
6. Y.R. Lee, A.V. Raghu, H.M. Jeong, and B.K. Kim, *Macromol. Chem. Phys.*, **210**, 1247 (2009).
7. A.V. Raghu, Y.R. Lee, H.M. Jeong, and C.M. Shin, *Macromol. Chem. Phys.*, **209**, 2487 (2008).
8. N.E. Marcovic, M.L. Auad, N.E. Bellesi, S.R. Nutt, and M.I. Aranguren, *J. Mater. Res.*, **21**, 870 (2006).
9. N. Soykeabkaew, P. Supaphol, and R. Rujiravanit, *Carbohyd. Polym.*, **58**, 53 (2004).
10. N.E. Marcovich, M.M. Reboredo, and M.I. Aranguren, *J. Appl. Polym. Sci.*, **70**, 2121 (1998).
11. X. Cao, H. Dong, and C.M. Li, *Biomacromolecules*, **8**, 899 (2007).
12. G.-X. Chen and H. Shimizu, *Polymer*, **49**, 943 (2008).
13. Q. Wu, M. Henriksson, X. Liu, and L.A. Berglund, *Biomacromolecules*, **8**, 3687 (2007).
14. M. Paillet and A. Dufresne, *Macromolecules*, **34**, 6527 (2001).
15. A. Dufresne and M.R. Vignon, *Macromolecules*, **31**, 2693 (2008).
16. M.A. Mosiewicki, G.A. Dell'Arciprete, M.I. Aranguren, and N.E. Marcovich, *J. Comp. Mat.*, **43**, 3057 (2009).
17. M.A. Mosiewicki, U. Casado, N.E. Marcovich, and M.I. Aranguren, *Polym. Eng. Sci.*, **49**, 685 (2009).
18. U. Casado, N.E. Marcovich, M.I. Aranguren, and M.A. Mosiewicki, *Polym. Eng. Sci.*, **49**, 713 (2009).
19. A. Bismarck, S. Mishra, and T. Lampke, *Natural Fibers, Biopolymers, and Biocomposites*, A.K. Mohanty, M. Misra, and L.T. Drzal, Eds., CRC Taylor & Francis, Boca Ratón, Chapter 2, 41 (2005).
20. M.A. Mosiewicki, J. Borrajo, and M.I. Aranguren, *Polym. Int.*, **54**, 829 (2005).
21. J.K. McKenzie, *Proc. Phys. Soc.*, **B63**, 2 (1950).
22. S.S. Narine, X. Kong, L. Bouzidi, and P. Sporns, *J. Am. Oil Chem. Soc.*, **84**, 55 (2007).
23. N.E. Marcovich, M.M. Reboredo, and M.I. Aranguren, *Thermochim. Acta*, **372**, 45 (2001).
24. M.A. Mosiewicki, G.A. Dell'Arciprete, M.I. Aranguren, and N.E. Marcovich, *J. Comp. Mat.*, **43**, 3057 (2009).
25. K.P. Somani, S.S. Kansara, N.K. Patel, and A.K. Rakshit, *Int. J. Adh. Adh.*, **23**, 269 (2003).
26. A.V. Raghu, G.S. Gadaginamath, H.M. Jeong, N.T. Mathew, S.B. Halligudi, and T.M. Aminabhavi, *J. Appl. Polym. Sci.*, **113**, 2747 (2009).